

How Useful are Conventional I -Vs for Performance Calibration of Single- and Two-Junction Perovskite Solar Cells? A Statistical Analysis of Performance Data on ≈ 200 Cells from 30 Global Sources

Tao Song,* Daniel J. Friedman,* and Nikos Kopidakis*

As perovskite photovoltaics (PV) advance from the laboratory to commercial prototypes, their accurate and reliable performance testing is becoming increasingly important. The well-documented dynamic response of perovskite solar cells to an external applied voltage has led to the development of steady-state performance measurement methods; however, these methods have not been widely adopted by the perovskite PV community. A key reason for this is that steady-state measurement methods take tens of minutes to complete, as opposed to conventional “fast” current–voltage (I - V) measurements usually lasting a few seconds. Fast I -Vs arise from a snapshot, almost always not a steady-state condition of the device; however, given their widespread use, the question arises: how do performance parameters of perovskite PV compare when measured with fast I - V and with a steady-state method? Results compiled from approximately 200 perovskite PV cells, including single junction, and two-terminal perovskite–perovskite and perovskite–Si tandems, show that fast I -Vs can provide a useful measure of the open-circuit voltage of the devices, while the short-circuit current and the overall efficiency can be widely misestimated. The implications of these findings on performance testing protocols are discussed and possible options for fast and accurate testing of perovskite PV are proposed.


1. Introduction

Perovskite solar cells have made remarkable strides in efficiency and are rapidly progressing from the research laboratory to commercial prototypes.^[1–3] Intense research has focused on thin film perovskite cells and, more recently, small modules. In addition, tandem cell architectures of perovskites on silicon and two-junction perovskite–perovskite are very active areas of research

and development. Research on these unconventional photovoltaic (PV) devices has also focused on accurate methods to characterize their performance under illumination. Perovskite PV exhibit a slow response of the photocurrent to an applied voltage; therefore, conventional current–voltage (I - V) scans with a predetermined, fixed voltage scan rate (typically 50–200 mV s^{−1}), do not measure the steady-state performance. In the remainder of the manuscript, we will refer to conventional I - V scans with preset voltage scan rate as “fast I - V .” Changes in perovskite devices under applied voltage typically take place over minutes and sometimes much longer, leading to the well-documented dependence of the I - V curve on voltage scan rate and scan direction.^[4–10]

These findings have led to the development of so-called steady-state performance measurement techniques aiming at bringing the device to a stable steady-state condition prior to recording its current and voltage. There are essentially two types of steady-state measurements (with some authors subdividing these into finer categories and/or using the terminology of “dynamic I - V ” to represent what we here call asymptotic I - V ^[7]). The first is the Asymptotic P_{MAX} , or Asymptotic I - V , where the device under test (DUT) is held at a constant voltage until the output current is stable to within preset criteria (usually a given percentage of current change per minute); when the stability criterion is reached the current is recorded and the DUT is biased to the next voltage.^[8] This way a partial I - V , typically around the maximum power point, is measured and the stabilized maximum power output, P_{MAX} , extracted, as shown in the example of Figure 1. The stabilized short-circuit current, I_{SC} , and open-circuit voltage, V_{OC} , are also extracted while the DUT is held at the short-circuit and open-circuit conditions, respectively. Figure 1 also shows a comparison of fast and asymptotic I - V scans measured for a typical 1-J perovskite cell, illustrating the differences observed between the two types of measurements. The second type of steady-state measurement is maximum power point tracking (MPPT), where a perturb-and-observe algorithm is used to keep the device at its maximum power point for a set period of time, then the average power is reported to represent the P_{MAX} of the device.^[9–11] These steady-state methods allow the device to

T. Song, D. J. Friedman, N. Kopidakis
PV Cell and Module Performance Group
National Renewable Energy Laboratory (NREL)
151313 Denver West Parkway, Golden, CO 80401, USA
E-mail: tao.song@nrel.gov; Daniel.Friedman@nrel.gov;
nikos.kopidakis@nrel.gov

 The ORCID identification number(s) for the author(s) of this article can be found under <https://doi.org/10.1002/solr.202100867>.

The publisher acknowledges that the United States Government retains a non-exclusive, paid-up, irrevocable, world-wide license to publish or reproduce the published form of this article, or allow others to do so, for United States Government purposes only.

DOI: 10.1002/solr.202100867

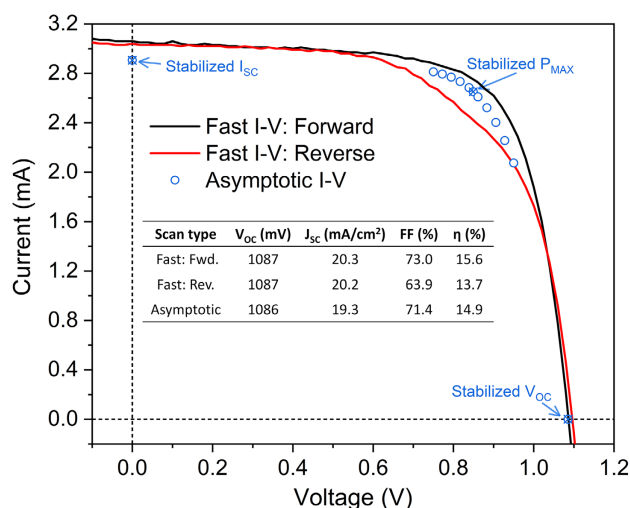


Figure 1. Fast I - V and asymptotic I - V scans of a perovskite solar cell. The fast I - V s are scanned in forward ($I_{sc} \rightarrow V_{oc}$) and reverse ($V_{oc} \rightarrow I_{sc}$) directions with the same scan rate of 100 mV s^{-1} . The Asymptotic I - V scan in this case lasted ≈ 20 mins (detailed scan procedure can be found in ref. [8]). The inset table lists the performance parameters obtained from these scans.

stabilize its output under continuous illumination, thereby obtaining a more reliable and (ideally) reproducible power rating than that obtained by a fast I - V scan. Recognizing the importance of steady-state power rating methods for perovskite PV, all major PV calibration laboratories use these methods when testing the performance of perovskite cells and modules, and the efficiency records reported in the solar cell efficiency tables^[2] are all measured with steady-state techniques.

Despite the problems posed by fast I - V s for power rating of perovskites, fast I - V s are still widely used in the perovskite R&D community, for several reasons. First, fast I - V is the default operating mode of any commercial solar simulator system. While steady-state methods do not require additional hardware, they do require modifications to the I - V scanning procedures, usually implemented in the measurement control software.^[8] Second, steady-state measurements take much longer, because of the stabilization criteria that the output current (or power) must fulfill. For example, an Asymptotic I - V measurement in our group takes a minimum of 10 min, during which the device is continuously exposed to 1 sun illumination. For a slow-responding device the asymptotic scan will take even longer. Hence, testing perovskite PV via steady-state methods a) makes the performance measurement a much lower throughput process than some laboratories require and b) is prohibitively slow in a production line testing environment. Additionally, some devices might encounter irreversible degradation during the test. Finally, a common argument in favor of fast I - V is that while it may not give an accurate power rating of a given perovskite device, it is still a useful tool for the relative comparison between devices. Hence, while the P_{MAX} extracted from the fast I - V of device A may not be accurate, if it is higher than the P_{MAX} of device B, then, the argument goes, device A will still be a better performer than device B when measured under steady-state conditions. The scope of this paper is to test this hypothesis, namely: what is the

correlation between the performance parameters, I_{sc} , V_{oc} , and efficiency (η) when measured with steady-state and with fast I - V ? Hence, to what extent can we use fast I - V for perovskite characterization? And lastly, are fast I - V s capable of providing reliable conclusions on the relative performance of perovskite devices?

Since 2017, the PV cell and module performance (CMP) group at NREL has received ≈ 200 perovskite solar cells, including 100 single-junction perovskite (hereafter termed 1-J PVSK), 45 perovskite/perovskite (PVSK/PVSK) and 50 perovskite/Si (PVSK/Si) monolithic two-junction cells, from over 30 global sources for performance certifications. All the cells were measured with the Asymptotic P_{MAX} scan method.^[8] In addition, two fast I - V s, in the forward and reverse direction, are also recorded prior to the asymptotic measurement. Using this protocol, two sets of cell performance parameters (i.e., unstabilized vs stabilized I_{sc} , V_{oc} , FF, P_{MAX} , and η) can be obtained from conventional fast I - V and the asymptotic P_{MAX} scans, respectively. Here, we conduct a detailed comparative analysis on the two sets of performance parameters based on the ≈ 200 perovskite devices received globally and discuss how useful conventional fast I - V scans are for performance calibration of perovskite devices. We find that fast I - V s generally overestimate J_{sc} and underestimate FF compared with the stabilized values obtained from asymptotic scans. For V_{oc} , the deviation between fast and asymptotic measurements is smaller, especially for the higher-voltage devices. For two-junction (2-J) PVSK/PVSK cells, the trends are comparable to 1-J PVSK cells. In contrast to those two classes of all-PVSK devices, 2-J PVSK/Si cells show a significantly better agreement between fast and steady-state I - V parameters. We quantify these results by linear regression analysis which can be easily used as a tool for evaluating the accuracy (and therefore the usefulness) of fast I - V s in more specific device subsets.

2. Experimental Section

To conduct an asymptotic P_{MAX} scan, two fast I - V scans—one each in the forward and reverse directions—are first performed on the DUT to indicate the magnitude of the hysteresis effect and help determine the voltage bias window for the asymptotic P_{MAX} scan. In our lab, the fast I - V scans usually take a few seconds with a typical scan rate of 100 mV s^{-1} . The unstabilized performance parameters such as I_{sc} , V_{oc} , P_{MAX} , and FF can be extracted from these scans accordingly. Then, the DUT is voltage-biased to a small set of voltages (usually 10) in the voltage bias window starting from the lower voltage limit, and each selected voltage bias is held constant until the current meets the stabilization criterion where the relative current change rate is smaller than $0.1\% \text{ min}^{-1}$ for 30 s. After the stabilized current for all voltage points has been obtained, a standard polynomial fitting algorithm is implemented to calculate the stabilized P_{MAX} as described in the relevant measurement standards.^[12,13] The stabilized I_{sc} and V_{oc} are each separately obtained after the P_{MAX} scan, using the same criteria when the cell is held at short-circuit and open-circuit conditions, respectively. An example dataset, including the two fast I - V s and the Asymptotic I - V scan is shown in Figure 1. The entire asymptotic P_{MAX} scan process normally takes about 10–20 mins for relatively stable devices. Optionally, the two fast I - V scans are repeated after the

asymptotic scan to check whether significant changes have occurred in the device response during the asymptotic scan. Unstable devices that did not reach our stabilization criteria are not included in the results below because no Asymptotic I - V data are available for them.

Note that all the performance results discussed here were measured at the standard test conditions (STCs), i.e., a device temperature of 25 °C, under the global hemispherical reference spectral irradiance, known as AM 1.5 Global (consisting of both direct and diffuse components incident on a 37° sun-facing tilted surface, giving rise to an Air Mass of 1.5), with a total irradiance of 1000 W m⁻² and a spectral irradiance distribution derived from a model of natural sunlight.^[14,15] This enables us to have a fair and meaningful comparative analysis between fast I - V and asymptotic measurements on different perovskite devices.

Finally, our benchmark measurement that we take to represent the true performance of the device at steady-state is the Asymptotic P_{MAX} scan because this method has been found to produce highly reliable results.^[7,8,16,17] As mentioned above, other steady-state measurement methods, such as MPPT, are also valid for performance rating of perovskite PV. Ultimately, the results we present below would have to be augmented to include comparison of fast I - V with other steady-state measurements in the perovskite and emerging PV community.

3. Results and Discussion

First, we give an overview of the performance deviation distribution on all the 200 perovskite cells received from over 30 global sources. Figure 2 shows the percentage deviation histograms of the V_{OC} , I_{SC} , FF, and η from fast I - V s compared with their steady-state values from asymptotic scans on these perovskite cells. The parameters from the fast I - V , hereafter denoted as “unstabilized” performance parameters, are normalized to their respective stabilized values obtained using the Asymptotic P_{MAX} method, and then subtracted from unity. The results are categorized with single-junction (“1-J”) perovskite (PVSK), two-junction (“2-J”) perovskite/perovskite (PVSK/PVSK), and 2-J perovskite/silicon (PVSK/Si) from left to right as shown in Figure 2a–c, respectively. From the histograms in Figure 2, we can observe at least three obvious performance deviation trends: 1) the deviations of all the performance parameters from the 2-J PVSK/Si cells are much smaller than those from the 1-J PVSK or the 2-J PVSK/PVSK cells, e.g., only ≈20% of the 2-J PVSK/Si cells having a relative η deviation larger than 1.5% as opposed to ≈80% of the other two types of cells and the deviation distribution range is much narrower as well; 2) for the 1-J PVSK and 2-J PVSK/PVSK cells, most of their J_{SC} deviation bins in Figure 2a,b distribute widely in the right side of the “0” deviation baseline

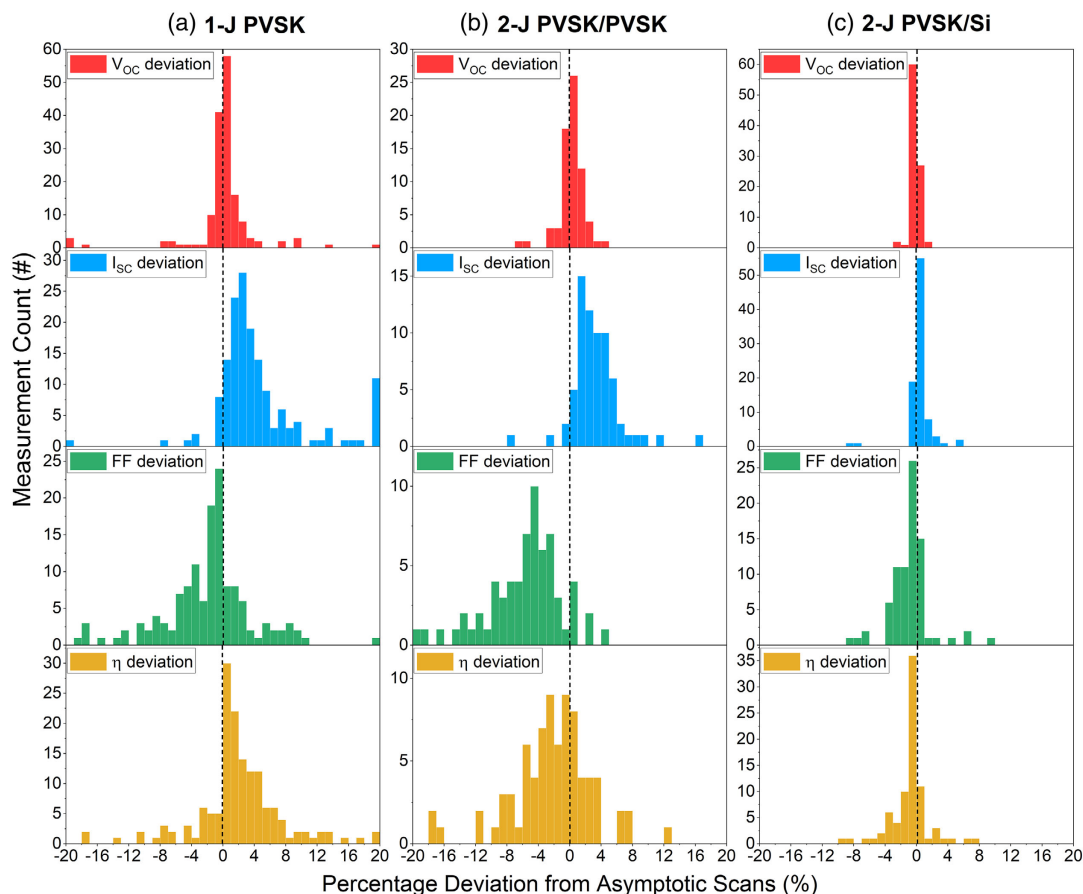


Figure 2. Percentage deviation of V_{OC} , I_{SC} , FF, and η from fast I - V s compared with asymptotic scans on ≈200 perovskite cells. Both forward ($I_{\text{SC}} \rightarrow V_{\text{OC}}$) and reverse ($V_{\text{OC}} \rightarrow I_{\text{SC}}$) scan results are presented, but not distinguished.

and hence the majority of the fast I - V scans generate higher J_{SC} values than asymptotic scans, i.e., $\approx 70\%$ of these cells giving at least 1.5% higher J_{SC} ; 3) in contrast to J_{SC} , a large fraction of 1-J PVSK and 2-J PVSK/PVSK cells (i.e., $\approx 50\%$ of 1-J PVSK and $\approx 90\%$ of 2-J PVSK/PVSK) have an underestimated FF over 1.5% with fast I - V scans.

We will give a more comprehensive explanation about these deviation trends in conjunction with the linear regression analysis on each performance parameter later. Note that we do not distinguish the scan directions (i.e., forward vs reverse) in the fast I - V results here. Their performance deviation trends do show dependence on scan directions in certain parameters, and a detailed discussion on them will be given in the following analysis for each type of cell as well. In the following analysis, we focus on the performance parameters that are most relevant to the physics of the device and the properties of the materials: V_{OC} (correlated to recombination mechanisms and to the bandgap of the perovskite) and J_{SC} (correlated to charge extraction efficiency, carrier mobility, and bandgap), extracted from fast I -Vs are often used to inform material and device development and to compare between device architectures. We discuss these parameters and their correlation with their respective stabilized values below. In addition, since the power conversion efficiency (η) is used extensively to assess developments within a solar cell technology and to compare between technologies, we also analyze the correlation of efficiencies extracted from fast I -Vs with the respective steady-state efficiency.

To find a more quantitative correlation between the unstabilized and stabilized parameters and make useful predictions and guidance for reliable performance measurements of perovskite PV devices, a linear regression analysis^[18] is conducted on the three types of perovskite cells based on their measured fast I - V and asymptotic scan datasets, respectively. Here, we set the reliable performance parameters from asymptotic scans as the best estimate of the true, steady-state value of that parameter and analyze the variation of the corresponding parameters from each cell's fast I -Vs, shown in the graphs as the dependent variable. For instance, **Figure 3** shows the measured fast I - V parameters (i.e., V_{OC} , J_{SC} , η) of 1-J PVSK solar cells as a function of their corresponding asymptotic values and their fitting curves based on the linear regression analysis. The red and blue dots represent the measured data points from forward and reverse fast I - V scans, respectively, and the red and blue lines are fits through

the corresponding data. Also calculated are the 95% prediction bands (lighter blue and red bands), which signify a 95% probability that, based on the existing observations, a future measured parameter from fast I - V will fall within this band. The dashed curve is the assumptive steady-state baseline with a slope of 1 and intercept of 0, so any points above the dashed curve have higher cell parameters in the fast I - V than the asymptotic values or vice versa. Given the relatively large sample size of ≈ 200 perovskite cells from over 30 global sources, the fitted curves along with their 95% prediction interval bands can quantify the strength of the relationship between the fast I - V and steady-state performance data and forecast a predictive performance deviation range of the fast I - V parameters of an unspecified perovskite cell based on existing observations.

In the following section, common trends of the performance deviation parameters (i.e., V_{OC} , J_{SC} , and η) for each cell type will be discussed with the linear regression analysis. Based on these quantitative findings, we will summarize useful implications and recommendations for perovskite device optimization and propose viable and reliable fast-screening parameters which can serve in a research lab or a production line more efficiently.

3.1. Single-Junction PVSK Cells

As shown in the histograms of Figure 2a, all the unstabilized performance parameters of the 1-J PVSK cells show deviation, to a degree dependent on the parameter of interest, from their steady-state parameters. We will discuss them with the more quantitative linear regression analysis here. In Figure 3a, the calculated 95% prediction band of unstabilized V_{OC} from fast I - V has an estimated deviation width (calculated as the vertical difference between the upper and lower end of the prediction band for a given $V_{OC,Asymp}$), $\Delta \widehat{V_{OC}} \approx \pm 30 - 60$ mV, dependent on where the measured V_{OC} is and which scan direction is chosen. The $\Delta \widehat{V_{OC}}$ is slightly larger for the forward scans than for the reverse scans. Overall, the fitted curves illustrate that the fast scans could give approximately same V_{OC} as the asymptotic scans but with a relatively large uncertainty $\approx 2-8\%$. Note that, in the 1.14–1.20 V region, the measured unstabilized V_{OC} points distribute more closely to both the fitted curves and the dashed baseline and the estimated V_{OC} deviation is $\approx 2\%$. In fact, all the cells in this region show high efficiency over 22% compared with

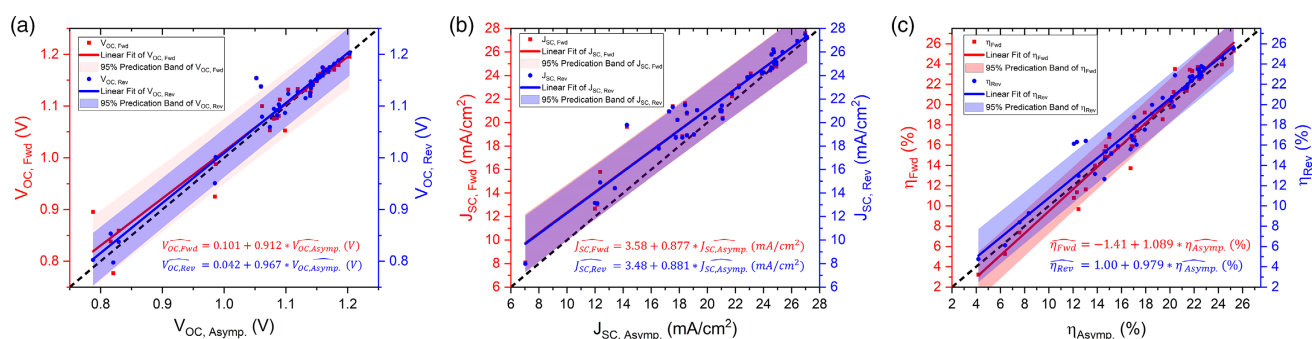


Figure 3. Measured unstabilized a) V_{OC} , b) J_{SC} , and c) η of 1-J PVSK cells from fast I - V scans (red: forward, blue: reverse) as a function of their corresponding asymptotic values; the red and blue curves and the bands are the fitted curves and prediction intervals from the linear regression analysis. The calculated linear equations from the regression analysis are also listed in the plots.

those cells with measured V_{OC} lower than 1.1 V and need a shorter time to obtain stabilized V_{OC} . One may infer that higher-efficiency and/or higher-bandgap 1-J PVSK cells with high V_{OC} could induce smaller performance discrepancy between fast and asymptotic scans, possibly caused by their faster-stabilizing dynamic response. Further details about the device configurations are necessary to confirm it.

In Figure 3b, the calculated linear equations from the forward and reverse scans have very similar slopes and intercepts and thus the fitted J_{SC} curves overlap with each other. Meanwhile, they both are above the assumptive steady-state baseline. As shown in the J_{SC} histogram in Figure 2a, $\approx 80\%$ 1-J PVSK cells have $>1.5\%$ (or $\approx 50\%$ cells $>3.5\%$) higher J_{SC} from fast I - V scans than from asymptotic scans. In other words, the J_{SC} of 1-J PVSK devices is very likely to be overestimated when extracted from fast I - V scans. Based on the linear regression analysis here, for instance, there is a 95% chance that a cell with a stabilized J_{SC} of 20 mA cm^{-2} will give a J_{SC} of $(21.1 \pm 1.2) \text{ mA cm}^{-2}$ when measured with fast I - V scans. Such a large J_{SC} overestimation, up to 11%, is nontrivial for a research lab and generates highly inaccurate performance comparisons of 1-J PVSK cells between different research groups. In short, the unstabilized J_{SC} value is not a reliable parameter for direct comparisons between different 1-J PVSK cells since there is a large chance that it could be overestimated. Perovskite researchers should therefore be cautious when using J_{SC} measured from fast I - V s as an indicator to guide device performance optimization.

In Figure 3c, the two fitted η curves from the forward and reverse scans diverge from each other, which can be seen in their calculated fitted equations as well. This divergence trend corresponds to the commonly seen hysteresis effect in 1-J perovskite cells. Such a divergence becomes more severe with poorer cell efficiency as shown in the 95% prediction bands. For cells with higher efficiencies, it is commonly observed that the hysteresis effect is less prominent. Due to the lack of device structures and fabrication methods on these cells, no further sound inferences could be drawn here. Meanwhile, we note that the width of η prediction bands for both the forward and reverse scans is large with an estimated $\Delta\hat{\eta} \approx \pm 2 - 3\%$ deviation from their stabilized η . Note that this deviation is in absolute percentage points. For instance, if a cell has a stabilized efficiency of 20%, there is a 95% possibility that its efficiency measured with a fast I - V scan could vary from 18% to 23%. With such a large measurement uncertainty, the fast I - V scans appear to be unable to provide trustworthy guidance for device optimization and comparison, particularly for those cells from different groups in which the fast I - V scan conditions vary.

Overall, both the measured and the predictive deviations between the unstabilized and stabilized performance parameters confirm that the fast I - V scan approach has apparent drawbacks for reliable comparison between different 1-J PVSK cells on their performance parameters, in particular on the J_{SC} . Note that the more-efficient cells could have as little as $\approx 1\%$ estimated $\Delta\widehat{V}_{OC}$ between fast and steady-state scans as shown in the upper right region in Figure 2a. Consequently, the V_{OC} parameter on these cells can probably serve as a good performance comparison indicator between cells. However, there is still a 95% chance that their stabilized efficiencies could be overestimated or

underestimated in a range of $\approx \pm 2-3\%$ (absolute) dependent on the scan directions and/or specific device properties if only fast I - V scans are performed. Later, we will discuss the limitation and usefulness of the fast scans in specific scenarios in Section 4.

3.2. Two-Junction PVSK/PVSK and PVSK/Si Cells

We now examine the performance deviations for two-junction ("2-J") PVSK/PVSK and PVSK/Si cells. The devices considered here are all two-terminal series-connected devices composed of top and bottom PV junctions connected optically and electrically by an interconnection layer. Ideally, the interconnection layer is perfectly electrically conducting, i.e., there is no voltage drop across the interconnection layer—a condition which is generally well approximated in practice. Therefore, we can consider the V_{OC} of the 2-J cells to be simply the sum of the top and bottom junction V_{OC} s, that is

$$V_{OC}^{PVSK/Si} = V_{OC}^{PVSK} + V_{OC}^{Si} \quad (1)$$

for PVSK/Si cells, and

$$V_{OC}^{PVSK1/PVSK2} = V_{OC}^{PVSK1} + V_{OC}^{PVSK2} \quad (2)$$

for PVSK/PVSK cells.

The deviations between unstabilized and stabilized V_{OC} measurements for these 2-J devices are shown in the V_{OC} deviation histograms in Figure 2b,c. These datasets show that the V_{OC} performance deviation is significantly less for the 2-J PVSK/Si (i.e., $\approx 95\%$ of them have a V_{OC} deviation within $\pm 0.5\%$ band) than for the 1-J PVSK cells or the 2-J PVSK/PVSK cells. This can be understood as resulting from the absence of performance deviation in the silicon cells: $\Delta V_{OC}^{Si} = 0$, so

$$\frac{\Delta V_{OC}^{PVSK/Si}}{V_{OC}^{PVSK/Si}} = \frac{\Delta V_{OC}^{PVSK}}{V_{OC}^{PVSK} + V_{OC}^{Si}} < \frac{\Delta V_{OC}^{PVSK}}{V_{OC}^{PVSK}} \quad (3)$$

A more quantitative view of the V_{OC} deviation between fast and steady-state measurements on these tandem cells is illustrated in Figure 4a and 5a. Regardless of scan directions, nearly all the measured unstabilized V_{OC} points from 2-J PVSK/Si cells lie closely to the assumptive steady-state baseline as shown in Figure 5a. There is only an estimated $\Delta\widehat{V}_{OC} \approx \pm 15 \text{ mV}$ from the steady-state V_{OC} points based on the 95% prediction interval bands, that is, $\approx \pm 0.6-0.9\%$ relative deviation from the assumptive steady-state baseline. The higher the unstabilized V_{OC} the smaller the relative deviation observed from the regression analysis. In contrast, as shown in Figure 4a, the unstabilized V_{OC} prediction bands from both directions are wider for 2-J PVSK/PVSK cells (i.e., $\Delta\widehat{V}_{OC} \approx \pm 40 - 120 \text{ mV}$ or $\approx \pm 2-6.9\%$ relative to its baseline; the specific $\Delta\widehat{V}_{OC}$ depends on the scan direction and the measured V_{OC}). In other words, there is a higher chance that the unstabilized V_{OC} parameter from a fast I - V scan is closer to the stabilized V_{OC} for 2-J PVSK/Si than for PVSK/PVSK cells. Additionally, we can observe from Figure 4a that the reverse fast scans for the 2-J PVSK/PVSK cells have a fitted curve closer to the baseline and narrower V_{OC} prediction bands. Therefore, if only fast I - V scans are applicable on this type of cells, a reverse fast

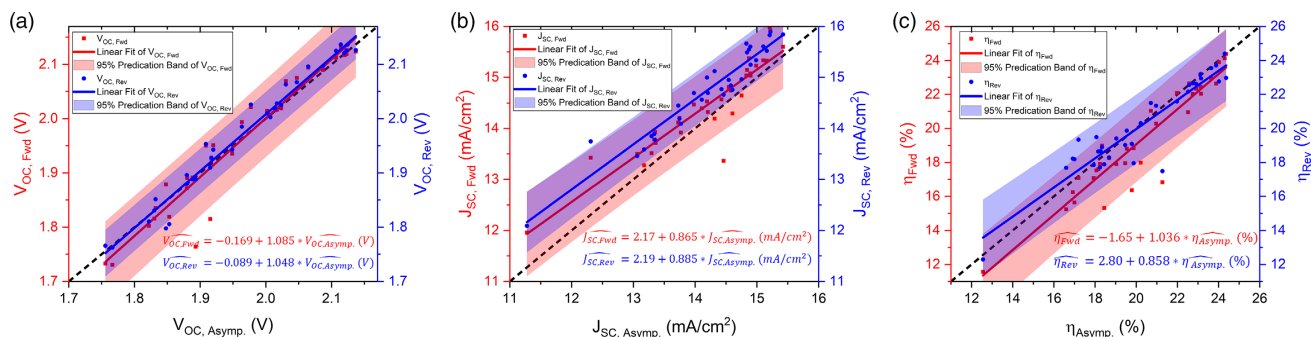


Figure 4. Measured unstabilized a) V_{OC} , b) J_{SC} , and c) η of 2-J PVSK/PVSK cells from fast I - V scans (red: forward, blue: reverse) as a function of their corresponding asymptotic values; the red and blue curves and the bands are the fitted curves and prediction intervals from the linear regression analysis. The calculated linear equations from the regression analysis are also listed in the plots.

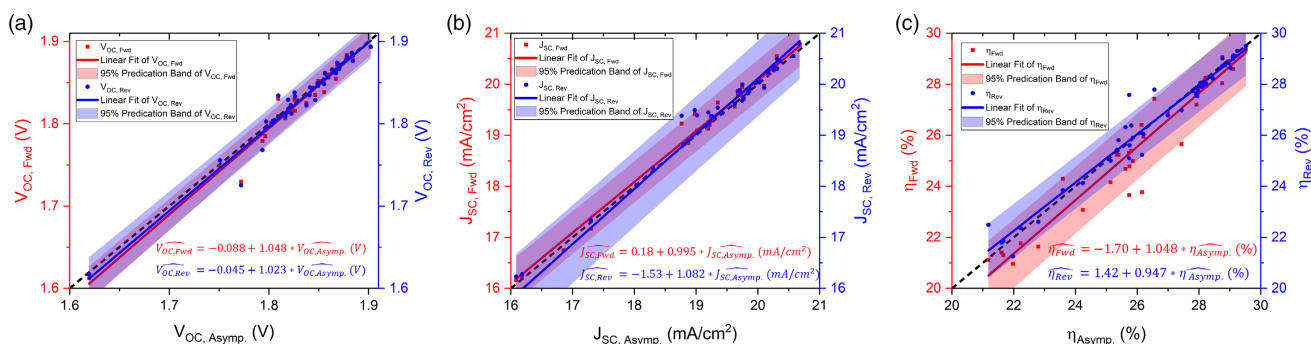


Figure 5. Measured unstabilized a) V_{OC} , b) J_{SC} , and c) η of 2-J PVSK/Si cells from fast I - V scans (red: forward, blue: reverse) as a function of their corresponding asymptotic values; the red and blue curves and the bands are the fitted curves and prediction intervals from the linear regression analysis. The calculated linear equations from the regression analysis are also listed in the plots.

I - V scan would be preferable for V_{OC} comparison since it produces lower discrepancy between the unstabilized and the stabilized V_{OC} s.

Turning our attention now to the J_{SC} performance deviation, Figure 2 shows that the J_{SC} performance deviation is significantly less for the 2-J PVSK/Si than for the 1-J PVSK cells or the 2-J PVSK/PVSK cells, that is, $\approx 19\%$ of 2-J PVSK/Si cells versus $\approx 80\%$ of 1-J PVSK and PVSK/PVSK have positive deviation $> 1.5\%$. This trend can again be traced to the absence of performance deviation in the silicon subcells, but the detailed explanation is different than for V_{OC} . In general, the J_{SC} of a series-connected multijunction cell is limited to be the lesser of the J_{SC} s of the individual junctions.^[19] For 2-J PVSK/Si cells whose stabilized J_{SC} is limited by the silicon junction, any positive deviation in the perovskite J_{SC} would not lead to a deviation in the 2-J J_{SC} . For 2-J PVSK/Si cells whose stabilized J_{SC} is instead limited by the perovskite junction, a positive deviation in the perovskite J_{SC} would lead to a positive deviation for the tandem, but that deviation would eventually be limited by the silicon J_{SC} . As shown in Figure 5b, most measured unstabilized J_{SC} points distribute very tightly close to the steady-state J_{SC} baseline for 2-J PVSK/Si cells, and over 80% of them have a slightly positive J_{SC} deviation smaller than 1%. Meanwhile, we can observe that comparing to the reverse scans, the forward scans give a better fitted curve with a narrower 95% prediction band with a slope of 0.995, an intercept of 0.15 mA cm⁻², and an estimated $\Delta J_{SC} \approx \pm 0.3$ mA cm⁻². In other words, the unstabilized

J_{SC} of a 2-J PVSK/Si cell extracted from a forward fast I - V scan would agree with its stabilized J_{SC} to within a narrow range of ± 0.3 mA cm⁻². In contrast, for 2-J PVSK/PVSK cells, nearly all the measured fast J_{SC} data in Figure 4b show higher values than the asymptotic scans and thus the fitted J_{SC} curves locate above the stabilized J_{SC} baseline. This positive J_{SC} deviation trend is similar to what we have observed in 1-J PVSK cells. Furthermore, the fitted J_{SC} curves show that the forward scans tend to give less J_{SC} overestimation compared to the reverse scans. For instance, if a 2-J PVSK/PVSK cell had a measured stabilized J_{SC} of 14.0 mA cm⁻², there is a 95% possibility that its unstabilized J_{SC} s from the forward and reverse scans would be 14.3 ± 0.7 and 14.6 ± 0.5 mA cm⁻², respectively. In summary, the J_{SC} deviation for the 2-J PVSK/Si cells is estimated to be much smaller than for the 1-J PVSK or the 2-J PVSK/PVSK cells due to the limitation of the Si subcell. Considering the high probability of J_{SC} overestimation from fast I - V scans on the latter two types of cells, researchers should take caution when using their unstabilized J_{SC} values to guide device optimization.

Lastly, we consider the η performance deviation. The η histograms in Figure 2 show that there is much less η deviation for the 2-J PVSK/Si than for the 1-J PVSK cells or the 2-J PVSK/PVSK cells. We can again understand this difference because of the absence of performance deviation in the silicon subcell, similar to the situation at V_{OC} . The voltage $V^{PVSK/Si}(J)$ of the 2J PVSK/PVSK device at any point along the J - V curve, including at the maximum-power current J_{max} , is the sum of the Si and PVSK

junction voltages, $V^{\text{PVSK/Si}}(J_{\text{max}}) = V^{\text{PVSK}}(J_{\text{max}}) + V^{\text{Si}}(J_{\text{max}})$. The current deviation is also much less due to the current limitation of the Si subcell. Therefore, by the same reasoning as applied above to V_{OC} , the absence of performance deviation in $V^{\text{Si}}(J_{\text{max}})$ means that the P_{max} or η performance deviation in 2J PVSK/Si cells can be expected generally to be less than for 1-J PVSK or 2-J PVSK/PVSK cells. Note that the areas of the devices from our customers span from $\approx \text{mm}^2$ to $\approx \text{cm}^2$ range and thus their P_{MAX} vary significantly from each other. Therefore, here we choose η rather than P_{MAX} to conduct the linear regression analysis. Figure 4c and 5c shows the unstabilized device efficiencies from fast scans as a function of the stabilized efficiencies from asymptotic scans and the linear fitted η curves for the 2-J PVSK/PVSK and PVSK/Si cells, respectively. First, we can observe that the fitted η curves between the forward and reverse scans diverge at lower efficiency for both types of cells, which is similar to the fitted η curves in the 1-J PVSK cells. This can be explained by the commonly seen I - V hysteresis effect in perovskite cells. The divergence is smaller for 2-J PVSK/Si than for PVSK/PVSK, due to the absence of performance deviation in the Si subcells. Additionally, nearly all the measured unstabilized η data from the forward scans locate below the baseline for both types of cells. Consequently, the forward fitted η curves (red-color) also lie below the assumptive steady-state baseline. In other words, forward fast I - V scans are more likely to underestimate the steady-state efficiencies for these cells. Overall, a steady-state efficiency measurement approach such as the asymptotic P_{MAX} scan is always the best way to extract reliable device efficiencies for 2-J cells. But if only rapid screening is applicable in a research facility, a reverse fast I - V scan is preferable to a forward scan for these cells. Next, we will give specific recommendations on performance calibration approaches with three application scenarios based on the linear regression analysis in this section.

4. Implications and Recommendations for Future Work

In the previous section, we have observed multiple performance deviation trends between the fast and the asymptotic scans on the three types of perovskite cells. The results presented above demonstrate the limitations of fast I - V characterization for perovskite devices, but also suggest applications for which fast I - V may be useful if appropriately conducted and interpreted. We frame the following discussion around three different applications for fast I - V .

4.1. Calibrated Low-Uncertainty Performance Measurements

It is well-known that perovskites have a dynamic response therefore stabilized measurements are necessary for perovskite solar cells. For the purpose of obtaining low-uncertainty calibrations of the complete I - V curve, the results presented here and elsewhere confirm the crucial role of stabilized measurements of slow-responding devices such as the perovskites.^[3–11] Nonetheless, fast I - V s do still have utility in this application, for providing a starting point for the V_{max} search in the stabilized measurement, and for checking for whether degradation occurred during the stabilized scan by doing fast I - V s before and after.^[8,16,17]

The steady-state efficiency measurement approaches (i.e., the asymptotic P_{MAX} scan and the maximum-power point tracking methods) are a must if researchers aim to obtain reliable performance calibration on their perovskite cells. Furthermore, if a world-record perovskite cell is expected from a research lab, we highly recommend sending it to an accredited PV testing group for official performance calibration. All these accredited testing centers have adopted the steady-state efficiency measurement protocol, and continuously invest in specialized equipment and expertise for high-precision PV performance calibration.

4.2. Device Research and Development

As discussed above, the V_{OC} values extracted from fast I - V tend to correlate quite well with the stabilized V_{OC} . In a perovskite device research and development environment, V_{OC} may thus be a useful performance metric to facilitate rapid-turnaround device development and/or Design of experiments studies of large numbers of devices. However, the value of the time saved by fast versus stabilized measurements is probably minor even in such circumstances. The main driver for using fast measurements in device R&D is more likely in facilitating the measurement of devices with insufficient stability to be measurable under stabilized conditions. Additionally, a strong recommendation from our results is that the unstabilized J_{SC} from fast I - V should not be considered as a trustworthy metric of device performance, even for device R&D applications where accuracy may be less critical than for certified calibrations.

Overall, considering that the best efficiencies of perovskite cells are already on par with conventional Si cells or even higher when utilizing tandem structures, researchers should be encouraged to deliver reliable efficiency results measured with steady-state measurement approach rather than to chase potentially highly unreliable results by taking advantage of short duration time in fast I - V scans. In the long run, with more researchers adopting steady-state measurements, there will be more efforts devoted into the improvement of device stability and in return, it will facilitate the success of perovskite PV technology in commercialization.

4.3. Quality-Control Screening on Manufacturing Line

PV manufacturing lines use high-speed measurement for quality-control screening, and to bin cells by power and current output. These measurements are done with flash testers which acquire the I - V data in a small fraction of a second, as required on a production line where even the few seconds of what we refer to here as a “fast” scan is unacceptably long. Because the devices tested on a production line are nominally identical, which is a very different and far more uniform population than the devices whose data are presented here, it is conceivable that performance parameters measured by flash I - V could be closely enough correlated with the stabilized performance parameters for flash I - V to retain its role as a screening and binning tool. But at minimum, the flash-stabilized performance correlations would have to be carefully developed and validated by a large number of stabilized measurements.

However, the results presented here and elsewhere^[20] suggest extreme caution in such an approach, especially in the use of P_{MAX} and J_{SC} metrics. Our results do suggest that more confidence is warranted in the use of V_{OC} . The V_{OC} segment of the fast I - V scans used here typically only takes 100 ms, which may be acceptable for production line testing. Such a procedure of using V_{OC} would still need to be backed by an initial calibration study for each device design, measuring rapid versus stabilized parameters to determine a predictive correlation between the two; and regularly thereafter, a practice of recurring steady-state measurements to validate that the correlation is still valid.

2-J PVSK/Si cells may prove more amenable than 1-J PVSK or 2-J PVSK/PVSK to the use of rapidly-measured J_{SC} and P_{MAX} as production line performance parameters. As discussed above, the performance parameters of 2Js whose current is limited by the Si junction will tend to be determined by that junction, with the consequence that rapid performance measurements of not just V_{OC} but also J_{SC} and P_{MAX} will be much better correlated with the steady-state measurements than for a 1-J PVSK or 2-J PVSK/PVSK. In practice, manufacturers may prefer such Si-current-limited designs in order to minimize performance degradation from beginning to end of life. An additional potential benefit to such a strategy, therefore, would be that it would tend to make J_{SC} (in addition to V_{OC}) a more trustworthy rapid screening parameter.

4.4. Recommendations for Future Work

We emphasize that our sample selection was not in any way controlled, i.e., we list and include in our analyses here all the cells that we have received and measured using the asymptotic P_{MAX} method. For example, as seen in Figure 3c, the efficiency of the PVSK devices in our dataset ranges from 4% to 24%, i.e., a very wide range and hence certainly a very wide distribution of device architectures. It is possible that the distributions of performance parameters from fast I - V presented here could become narrower if only subsets of “similar” devices were considered. Additionally, we did not vary the fast I - V scan conditions to explore the possibility of narrower prediction band widths. Our analysis is based on a constant (and typical) fast I - V scan rate of 100 mV s^{-1} , however, it remains to be seen if there are more optimal voltage scan rates for perovskite solar cells, or device preconditioning methods prior to I - V testing, that make fast I - V s accurate enough to meet specific performance calibration needs. With this in mind, the prediction interval analysis shown in Figure 3–5 can be used as a validation tool for individual perovskite PV laboratories to assess the accuracy of fast I - V measurement protocols for their devices under their measurement conditions.

Finally, the relatively simple linear regression analysis with prediction intervals presented here and applied only to V_{OC} , J_{SC} , and η for reasons discussed above can be applied to additional parameters of interest in a solar cell performance calibration. In particular, the FF, being a compound parameter affected by V_{OC} , J_{SC} , and P_{MAX} , was less discussed in our analysis above. We observed that most of the perovskite cells measured with fast I - V scans show underestimated FFs compared with their asymptotic scans in Figure 2. However, the linear regression analysis of

FF extracted from fast I - V and from Asymptotic scans for the three types of solar cells discussed here shows a poor fit quality and therefore is of limited use for the wide and uncontrolled device selection used in this work (see Figure S1, Supporting Information). It would be interesting to re-evaluate the correlation of unstabilized to stabilized FF in subsets of cells with better controlled architectures (e.g., contacts).

In conclusion, we think these types of analyses will further the discussion of the usefulness of fast I - V characterization and could also provide additional Supporting Information toward the development of fast I - V testing methods for perovskite research labs and production facilities alike.

5. Conclusion

By comparing PVSK PV cell performance parameter values from fast versus steady-state I - V measurements for a wide range of cells, we identified and quantified trends that offer insights into the applicability and limits of fast I - V in understanding PVSK cell performance. The fast I - V s generally overestimate J_{SC} and underestimate FF compared with the asymptotic scans. For V_{OC} , the deviation between fast and asymptotic measurements is less, especially for the higher-voltage devices. For 2-J PVSK/PVSK cells, the trends are comparable to 1-J PVSK cells. In contrast to those two classes of all-PVSK devices, 2-J PVSK/Si cells show a significantly better agreement between fast and steady-state I - V parameters. This difference can be understood by the influence of the silicon bottom junction, for which there is effectively no distinction between fast and steady-state I - V , on the cell performance. On the basis of these results, we presented recommendations for when and how fast I - V s may have value in both R&D and manufacturing applications, and, correspondingly, when asymptotic I - V measurements must be used.

Supporting Information

Supporting Information is available from the Wiley Online Library or from the author.

Acknowledgements

The authors thank C. Mack and R. Williams for conducting part of the measurements, and all the customers who sent cells for performance certification. This work was authored by Alliance for Sustainable Energy, LLC, the manager and operator of the National Renewable Energy Laboratory for the USA. Department of Energy (DOE) under contract no. DE-AC36-08GO28308. Funding provided by U.S. Department of Energy Office of Energy Efficiency and Renewable Energy Solar Energy Technologies Office (SETO) Agreement No. 34351. The views expressed in the article do not necessarily represent the views of the DOE or the U.S. Government.

Conflict of Interest

The authors declare no conflict of interest.

Data Availability Statement

The data that support the findings of this study are available on request from the corresponding authors. The data are not publicly available due to privacy or ethical restrictions.

Keywords

linear regression analysis, performance calibration, perovskites, single and two-junction solar cells, tandem cells

Received: October 15, 2021

Revised: November 10, 2021

Published online: December 4, 2021

- [1] NREL, Best Research-Cell Efficiency chart, <https://www.nrel.gov/pv/cell-efficiency.html> (accessed: October 2021).
- [2] M. A. Green, E. D. Dunlop, J. Hohl-Ebinger, M. Yoshita, N. Kopidakis, X. Hao, *Prog. Photovoltaics* **2021**, 29, 657.
- [3] Y. Rong, Y. Hu, A. Mei, H. Tan, M. I. Saidaminov, S. I. Seok, M. D. McGehee, E. H. Sargent, H. Han, *Science* **2018**, 361, 6408.
- [4] H. J. Snaith, A. Abate, J. M. Ball, G. E. Eperon, T. Leijtens, N. K. Noel, S. D. Stranks, J. T. W. Wang, K. Wojciechowski, W. Zhang, *J. Phys. Chem. Lett.* **2014**, 5, 1511.
- [5] E. V. Unger, E. T. Hoke, C. D. Bailie, W. H. Nguyen, A. R. Bowring, T. Heumüller, M. G. Christoforo, M. D. McGehee, *Energy Environ. Sci.* **2014**, 7, 3690.
- [6] W. Tress, N. Marinova, T. Moehl, S. M. Zakeeruddin, M. K. Nazeeruddin, M. Grätzel, *Energy Environ. Sci.* **2015**, 8, 995.
- [7] R. B. Dunbar, B. C. Duck, T. Moriarty, K. F. Anderson, N. W. Duffy, C. J. Fell, J. Kim, A. Ho-Baillie, D. Vak, Y. Wu, K. Weber, A. Pascoe, Y.-B. Cheng, Q. Lin, P. L. Burn, R. Bhattacharjee, H. Wang, G. J. Wilson, *J. Mater. Chem. A* **2017**, 5, 22542.
- [8] T. Song, D. Friedman, N. Kopidakis, *Adv. Energy Mater.* **2021**, 11, 2100728.
- [9] G. Bardizza, H. Mülleijans, D. Pavanello, E. D. Dunlop, *J. Phys. Energy* **2020**, 3, 021001.
- [10] E. Zimmermann, K. K. Wong, M. Müller, H. Hu, P. Ehrenreich, M. Kohlstädt, U. Würfel, S. Mastroianni, G. Mathiazhagan, A. Hinsch, T. P. Gujar, *APL Mater.* **2016**, 4, 091901.
- [11] N. Pellet, F. Giordano, Dar M. Ibrahim, G. Gregori, SM Zakeeruddin, J. Maier, M. Grätzel, *Prog. Photovoltaics: Res. Appl.* **2017**, 25, 942.
- [12] IEC 60904-1: 2020, Photovoltaic devices – Part 1: Measurement of photovoltaic current-voltage characteristics 2020, <https://webstore.iec.ch/publication/32004> (accessed: October 2021).
- [13] ASTM E948-16, Standard Test Method for Electrical Performance of Photovoltaic Cells Using Reference Cells Under Simulated Sunlight 2020, <https://compass.astm.org/Standards/HISTORICAL/E948-15.htm> (accessed: October 2021).
- [14] ASTM G173-03, Standard Tables for Reference Solar Spectral Irradiances: Direct Normal and Hemispherical on 37° Tilted Surface, ASTM, Philadelphia, PA **2006**. [https://compass.astm.org/EDIT/html_annot.cgi?G173+03\(2020\)](https://compass.astm.org/EDIT/html_annot.cgi?G173+03(2020)) (accessed October 2021).
- [15] IEC 60904-3, Photovoltaic devices – Part 3: Measurement principles for terrestrial photovoltaic (PV) solar devices with reference spectral irradiance data 2019, <https://webstore.iec.ch/publication/61084> (accessed: April 2021).
- [16] T. Moriarty, D. Levi, *2017 IEEE 44th Photovoltaic Specialist Conf. (PVSC)*, IEEE, Washington, DC **2017**, pp. 483–486.
- [17] T. Song, T. Moriarty, D. Levi, *2019 IEEE 46th Photovoltaic Specialist Conf. (PVSC)*, Vol. 2, IEEE, Chicago, IL **2019**, pp. 1–5.
- [18] The linear regression analysis, https://www.originlab.com/doc/Origin-Help/LR-Algorithm#Simple_Linear_Regression_Model (accessed: October 2021).
- [19] D. J. Friedman, J. M. Olson, S. Kurtz, in *Handbook of PV Science And Engineering* (Eds: A. Luque, S. Hegedus), Vol. 2, John Wiley & Sons, Hoboken, NJ **2011**, ch. 8.
- [20] T. Song, L. Ottoson, J. Gallon, D. J. Friedman, N. Kopidakis, *2021 IEEE 48th Photovoltaic Specialist Conf. (PVSC)*, Vol. 2, IEEE, Virtual, **2021**, pp. 0367–0371.